SHORT-PERIOD (7-s TO 15-s) GROUP VELOCITY MEASUREMENTS AND MAPS IN CENTRAL ASIA

Anatoli L. Levshin,[2] Jeffry L. Stevens,[1] Michael H. Ritzwoller,[2] and David A. Adams [1]

Science Applications International Corporation,[1] University of Colorado at Boulder[2]

Sponsored by Defense Threat Reduction Agency

Contract No. DTRA01-00-C-0026

ABSTRACT

This research program is a joint project between the University of Colorado (CU) and SAIC. CU has measured a large number of surface wave dispersion curves for paths crossing central Asia. The data analysis has concentrated on short-period (7- to 15-s) measurements, which allow finer resolution than previous studies, which were performed at longer periods. The region studied includes western China, northern India, and Pakistan. Surface wave data have been obtained from more than 1600 events recorded on 240 stations of the GSN, GEOSCOPE, KNET, KAZNET, CDSN, GEOFON and MEDNET networks. In addition, data have been acquired from temporary PASSCAL networks in Saudi Arabia and Tibet. A total of 7,800 Rayleigh wave dispersion curves and 5,400 Love wave dispersion curves were recovered from the data. The Rayleigh wave dispersion measurements are organized into two groups. One group (65484 points) consists of one dispersion curve per ray path, while the other one (48590 points) is made up of summary dispersion curves found by averaging measurements made over similar paths. Two paths are defined as similar when their end points lie within 55 km of one another. In addition, Station-Specific Source Corrections (SSSC's) have been derived for Rayleigh waves at periods of 7-20 seconds for 50 International Monitoring System (IMS) acting and reserved stations. Both the dispersion data sets and SSSC's will be delivered to the Center for Monitoring Research (CMR) at the conclusion of the project.

SAIC's role in this project is to perform validation of CU's dispersion curves by testing them on IMS data at the CMR. This is being accomplished by reviewing the dispersion curves and comparing with both predicted values and other measurements along similar paths. Predictions made after incorporating the new data are then compared with a larger set of data including IMS data in addition to the input data. Predictions are made using a global earth model similar to the models used in the operational system at the International Data Centre (IDC). These models are developed by inversion of a large data set of dispersion measurements using a modification of the Crust 2.0 earth model over AK135 as a starting model. Dispersion curves calculated from the models are used for surface wave detection. The new dispersion curves being measured by CU are added to the global data set. The predictions of the model are used to perform an initial assessment of the validity of the measured dispersion curves, and then the measured dispersion curves are used to improve the models and the predicted dispersion curves. In our initial assessment of the effect of the higher frequency data on the earth models, we found that it was necessary to increase the number of crustal layers in the starting models and decrease their thickness in order to match the higher frequency dispersion data. New models were also required to match some difficult regions, such as the Tarim Basin, which strongly affect the surface wave dispersion curves. The final stage of validation will be to construct phase-matched filters from the predicted dispersion curves and then apply them to IMS data that were not part of the initial data set and assess the data compression and detection performance of the predictions.

OBJECTIVE

This research program is a joint project between the University of Colorado (CU) and SAIC. The primary objective is to measure and validate high-frequency (7-s to 15-s) surface wave dispersion curves and develop group velocity maps and earth models for Western/Central Asia, including Western China, North India, and Pakistan. The dispersion maps are then used to develop SSSC's and phase-matched filters to improve surface wave detection and measurement.

RESEARCH ACCOMPLISHED

In this project we develop improved group velocity dispersion curves and maps for West/Central Asia covering the region approximately from 10 to 50 degrees north latitude and 20 to 140 degrees east longitude. We refine existing dispersion curves; extend the curves to higher frequency (7- to 15-s period) and measure new dispersion curves. A total of 7,800 Rayleigh wave dispersion curves and 5,400 Love wave dispersion curves were recovered from the data.

Data

We acquired waveform data from IRIS DMC, GEOSCOPE and GEOFON data centers for the seismic events that occurred in 1996-2000. Altogether data from more than 1600 events recorded by about 260 stations of the GSN, GEOSCOPE, KNET, KAZNET, CDSN, GEOFON, MEDNET, and temporary PASSCAL networks in Saudi Arabia and Tibet have been acquired and analyzed. Figure 1 shows the locations of stations and events used in this study.

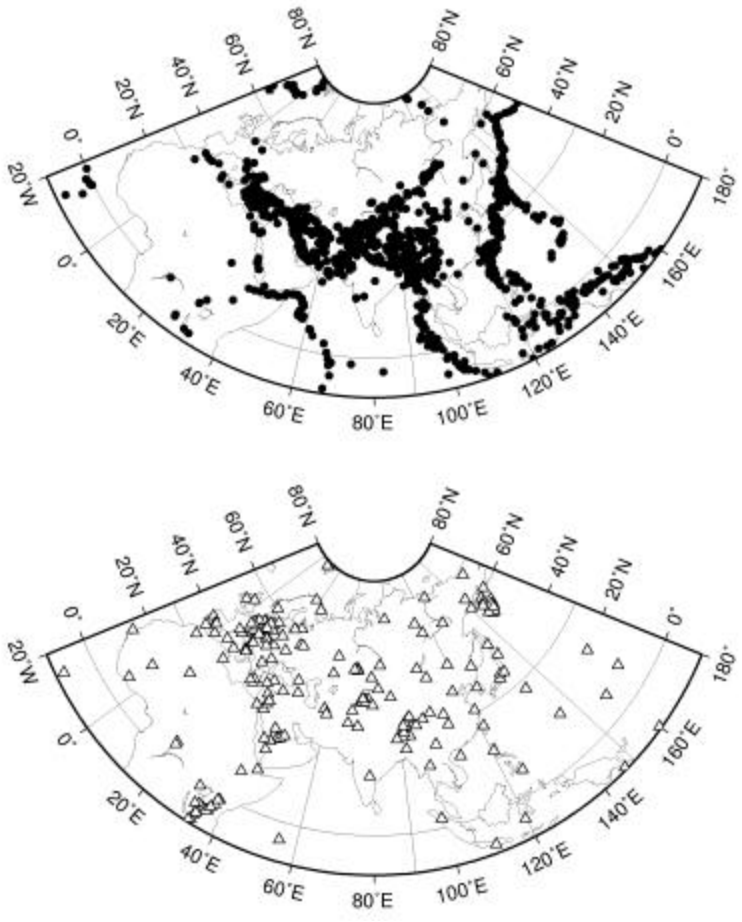

Figure 1. Locations of events (top) and stations (bottom) used in this study.

Surface wave dispersion measurements

Waveform data and accompanying information were converted into the CSS 3.0 format database. After preprocessing, these data were used for measuring group velocities of Rayleigh and Love waves in period range 7-15 s. All data were processed by seismic analysts in a semi-automatic regime using the frequency-time analysis package FTAN developed at CU (Dziewonski *et al*., 1968; Levshin *et al*., 1972; Russell *et al*., 1988; Levshin *et al*., 1992; Ritzwoller *et al*., 1995) to obtain group travel-time, phase travel-time, and spectral amplitude measurements. Group velocities and phase velocities were then computed from these travel times and distances between the receiver and the Harvard-CMT location (Dziewonski *et al*., 1981) when it existed, or, alternatively, the receiver and the PDE location. As part of FTAN, an analyst interactively designed a group velocity-period filter to reduce contamination from other waves and coda, chose the frequency band for each measurement, and assigned a qualitative grade (A - F) to each measurement. These new data were combined with an existing data set to form the input for tomographic inversion. Altogether, more than 7,800 dispersion curves of Rayleigh waves and 5,400 dispersion curves of Love waves were obtained.

Dispersion measurements were passed through several post-processing procedures for quality control. Evident outliers were rejected by comparison of observed travel times with predictions from reference group velocity maps corresponding to CU's recent global model (Shapiro and Ritzwoller, 2002). Then the measurements for close paths were combined into single common path measurements by averaging observed group velocities and rejecting outliers. The number of individual and declustered measurements as a function of period is shown in Figure 2. Declustering allows the accuracy of individual measurements to be estimated. RMS scatter of measurements at different periods is between 0.020-0.025 km/s both for Rayleigh and Love waves.

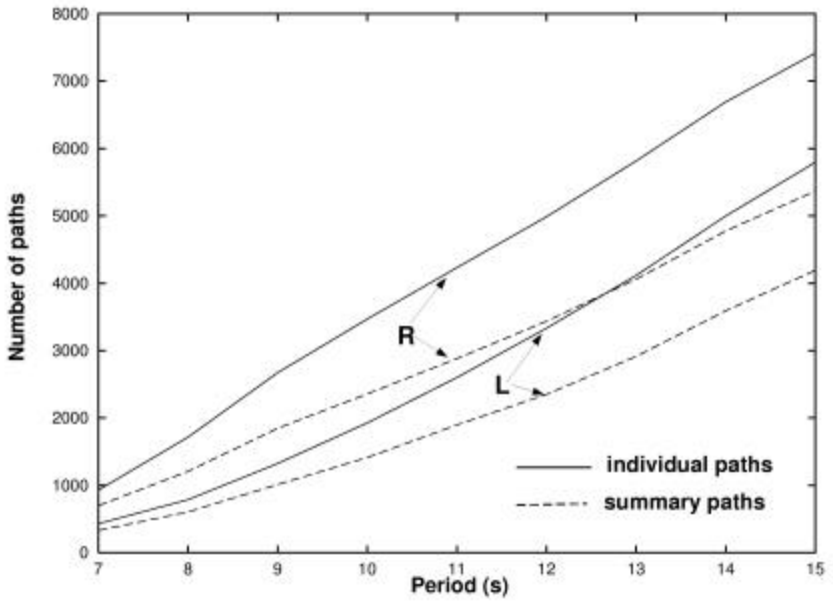

Figure 2. Number of individual and declustered measurements as a function of period for Rayleigh (R) and Love (L) waves.

The coverage of the studied region by surface wave observations varies geographically and with period. At 7 s almost all observations concentrate around KNET. At 15 s the path density is quite homogeneous across the region with an exception in Southern India. Maps of Rayleigh wave path density for several periods are shown in Figure 3.

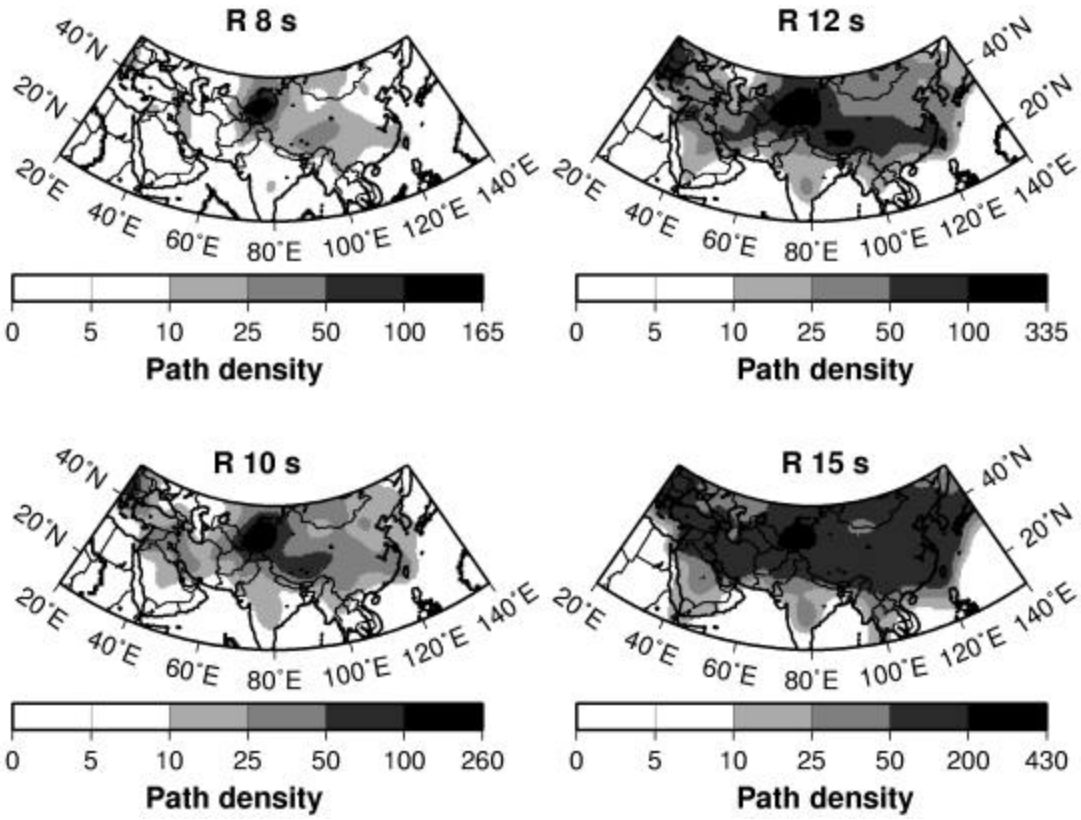

Figure 3. Rayleigh wave path density. Path density is defined as the number of paths crossing 2-degree cells.

CU Dispersion Maps and Station-Specific Source Corrections

Declustered data sets were converted to tomographic maps using the techniques described in Barmin *et al*. (2001). We produced tomographic group velocity maps for periods 7, 8, 9, 10, 11, 12, 13, 14, 15 s for Rayleigh and Love waves. As reference maps we used smoothed maps predicted by the CU global models (Shapiro and Ritzwoller, 2002). The resulting maps are accompanied by path density, resolution and amplitude bias maps, and differential maps characterizing additional signals contained in the new set of group velocity maps relative to the reference maps. The maps at 7 s are very close to the reference maps as the low density of observations penalizes perturbations relative to the initial model. As the period increases the difference between the initial maps and our tomographic maps becomes more and more significant, especially for Pakistan, Western China and N. India, indicating the presence of new information in the short-period data obtained in this study. Analysis of resolution maps demonstrates that spatial resolution changes from 300-400 km to 100-200 km with increasing period.

We calculated SSSCs for Rayleigh waves at periods of 7-20 s for 50 IMS acting and reserved stations. The SSSCs contain values of group velocity perturbation and travel time perturbation relative to the reference curve values on the one degree grid for a distance range of up to 30 degrees from the stations. An example of the SSSC for several periods is shown in Figure 4.

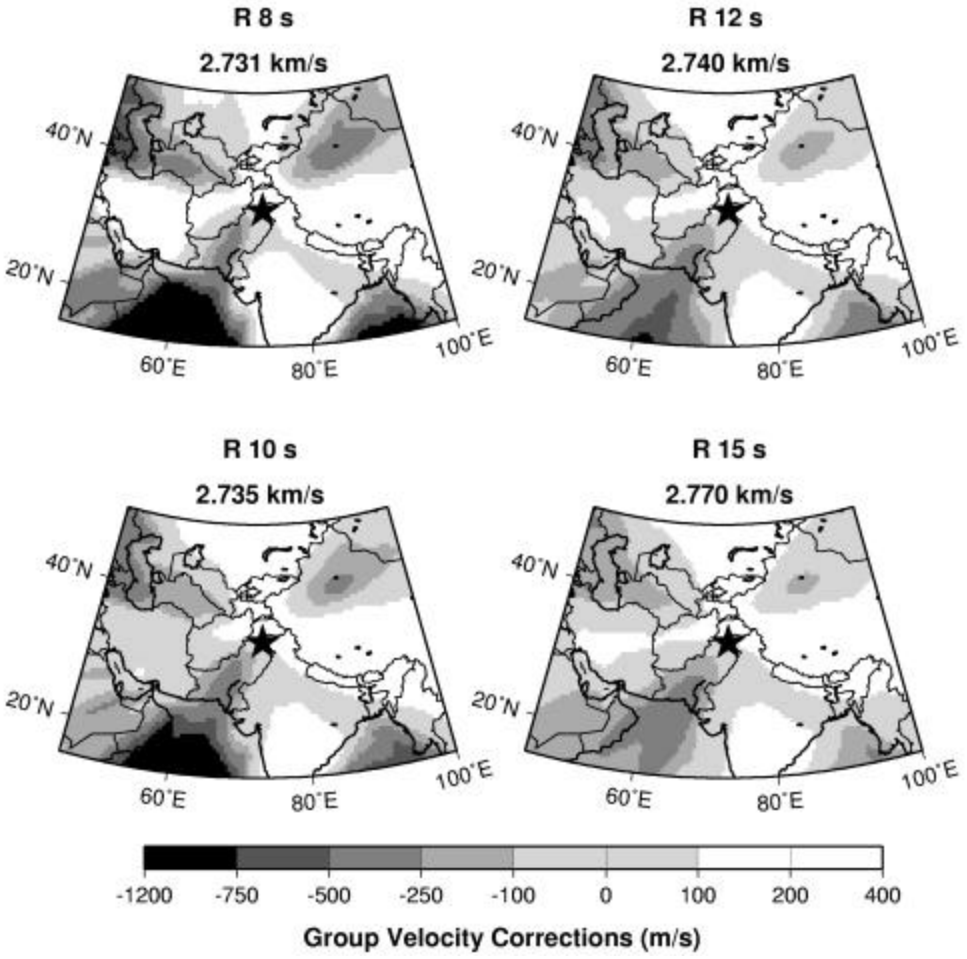

Figure 4. Rayleigh wave site-specific station corrections for station PAK0 at several periods. Values of reference velocities are shown above the maps.

Comparison of CU and SAIC dispersion maps

SAIC is performing validation of CU's dispersion curves by testing them on IMS data at CMR. This is being accomplished by reviewing the dispersion curves and comparing with both predicted values and other measurements along similar paths. Predictions made after incorporating the new data are then compared with a larger set of data, including IMS data in addition to the input data. Predictions are made using a global earth model similar to the models used in the operational system at the International Data Centre (IDC) (Stevens and McLaughlin, 2001). These models are developed by inversion of a large data set of dispersion measurements using a modification of the Crust 2.0 earth model (Laske, *et al*, 2001) over AK135 (Kennett *et al*, 1995) as a starting model (Stevens *et al*., 2002). Dispersion curves calculated from the models are used for surface wave detection. The new dispersion curves being measured by CU are added to the global data set. The predictions of the model are used to perform an initial assessment of the validity of the measured dispersion curves, and then the measured dispersion curves are used to improve the models and the predicted dispersion curves.

The SAIC dispersion maps are derived as described above by determining a set of earth structures and then calculating the dispersion. The CU maps in contrast are determined by inverting group velocity measurements to get group velocity maps for a set of periods without determining an earth model. The SAIC data set is a superset of the CU data set, incorporating other data for this region including dispersion curves derived from IMS data and explosions at the Shagan River and Novaya Zemlya test sites. Consequently, a comparison of the maps provides a good check on each. Figure 5 shows the SAIC and CU dispersion maps at periods of 10 and 20 seconds. Although there are some differences, in general they are in good agreement.

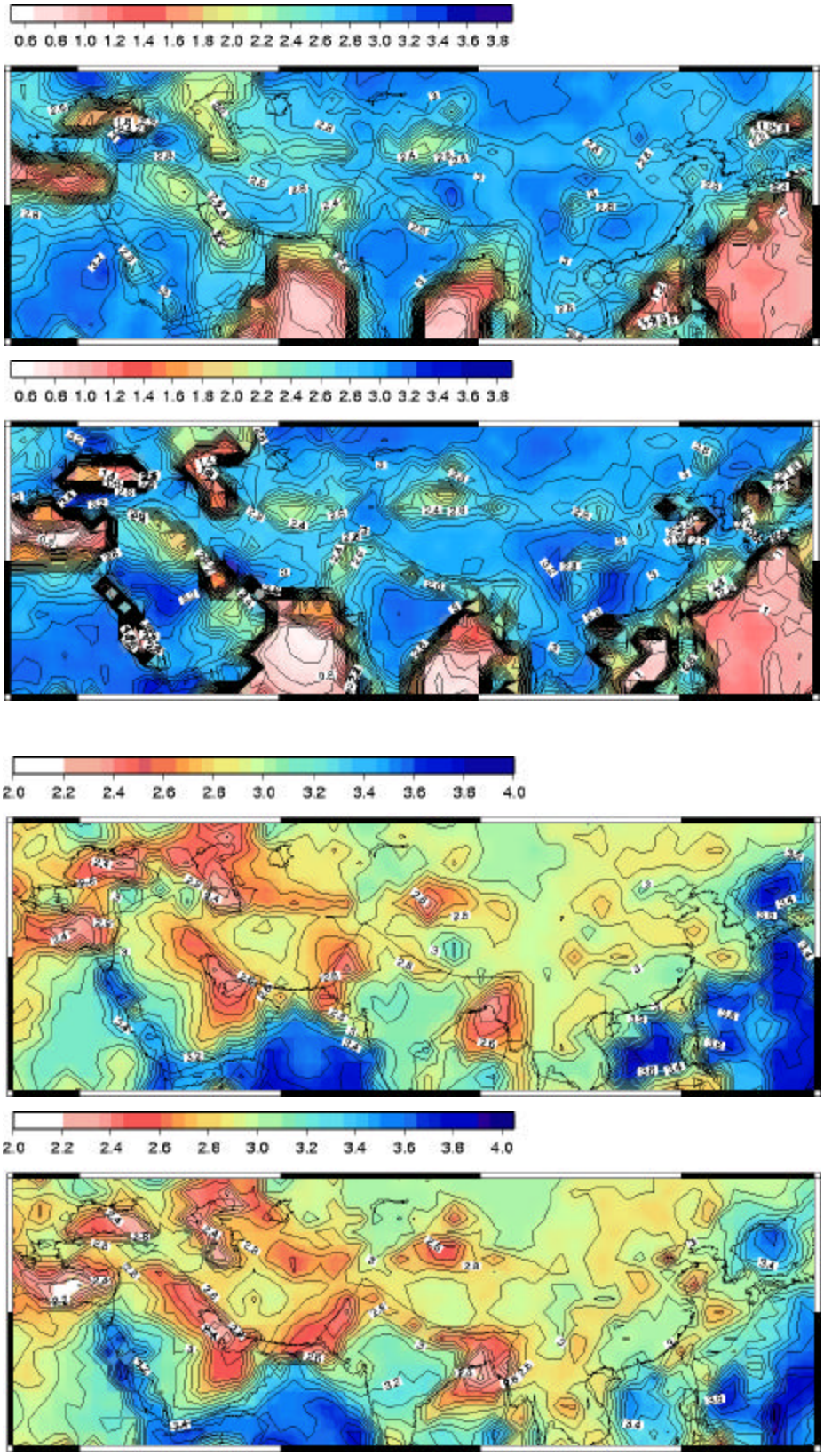

Figure 5. Group velocity maps for 10-s (top two maps) and 20-s (bottom two maps) period. Top map of each is derived using the SAIC procedure, bottom using CU procedure.

Tarim Basin group velocities

For most of the data set, we get good agreement between predicted and observed values after inversion. The Tarim Basin region in Western China, however, has proven to be difficult, so we discuss this area in some detail here. Most of the Tarim Basin data was recorded at the KNET array in Kyrgyzstan. Figure 6 shows raypaths of data recorded at this station in two frequency bands. The paths are color coded according to the slowness residual $1\text{-}s_o/s_p$ where s_o and s_p are the observed and predicted group slownesses. Blue paths indicate observed group velocity slower than predicted, red faster than predicted. In the low-frequency band (period>22 seconds), there is some variation in the residuals, but there are no large, consistent regions of data misfit. In contrast, in the high-frequency band of 0.08 to 0.15 Hz, there is a striking feature of blue rays centered in a southeast direction and passing through the Tarim Basin.

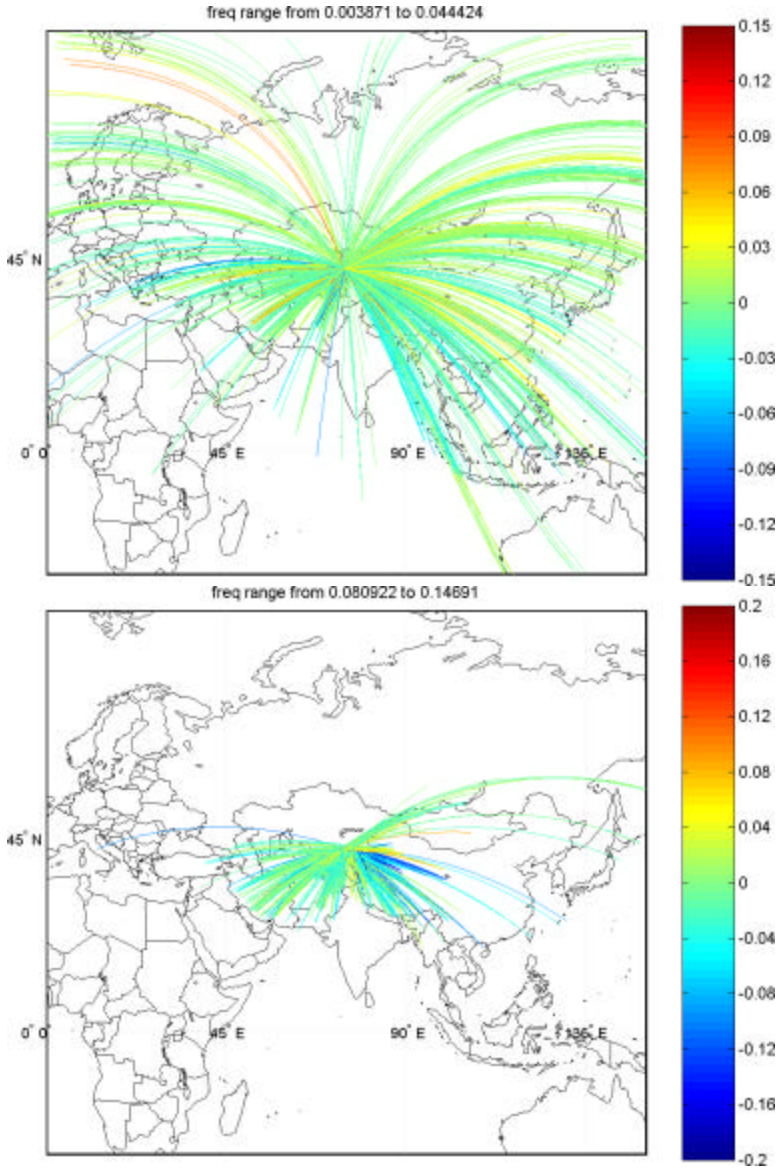

Figure 6. Paths color-coded according to residuals for group velocity dispersion curves for periods greater than 22 s (top) and for periods of 7-13 s (bottom) recorded at the station cluster in and near Kyrgyzstan.

Figure 7 shows the dispersion curves associated with these same paths. Notice the very wide range of group velocities at the higher frequencies, differing by as much as 40% over this narrow band of paths. The most northerly paths, which just skirt the Tarim Basin, are faster than the model, while the ones pointing more southerly are slower than the model.

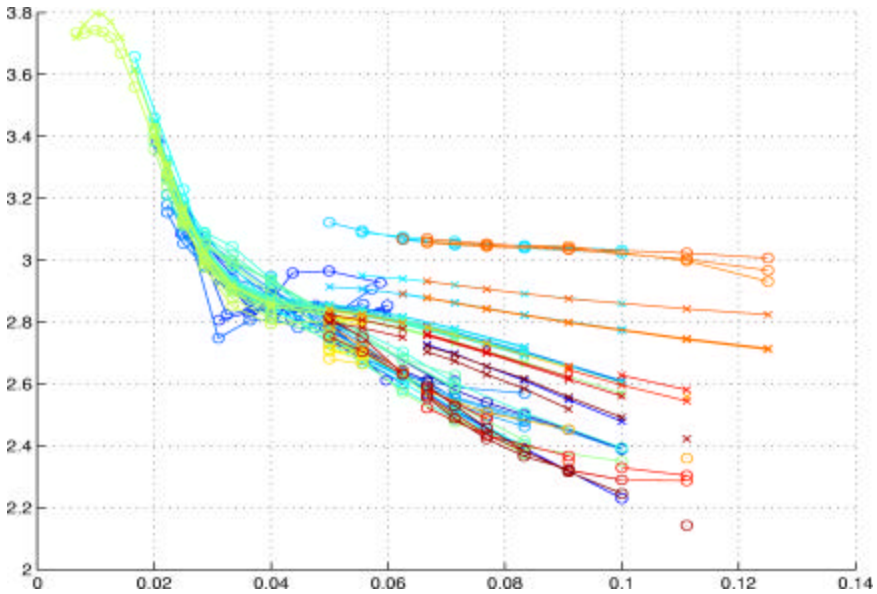

Figure 7. Group velocity dispersion curves recorded at the cluster of stations in the Kyrgyzstan cluster from sources located across the Tarim Basin. The "x"s and "o"s are predicted and observed velocities respectively. The colors are for cross-referencing between observed and predicted velocities and with the raypaths shown in Figure 8.

Figure 8 shows some of these paths plotted against the depth of sediments. The difficulty with these dispersion curves is caused by a geophysical effect – a large change in earth structure over a very small change in azimuth that causes a large change in high-frequency surface wave dispersion. In this case it is necessary to refine the model types and locations so that they accurately follow the basin boundary in order to be able to predict the dispersion.

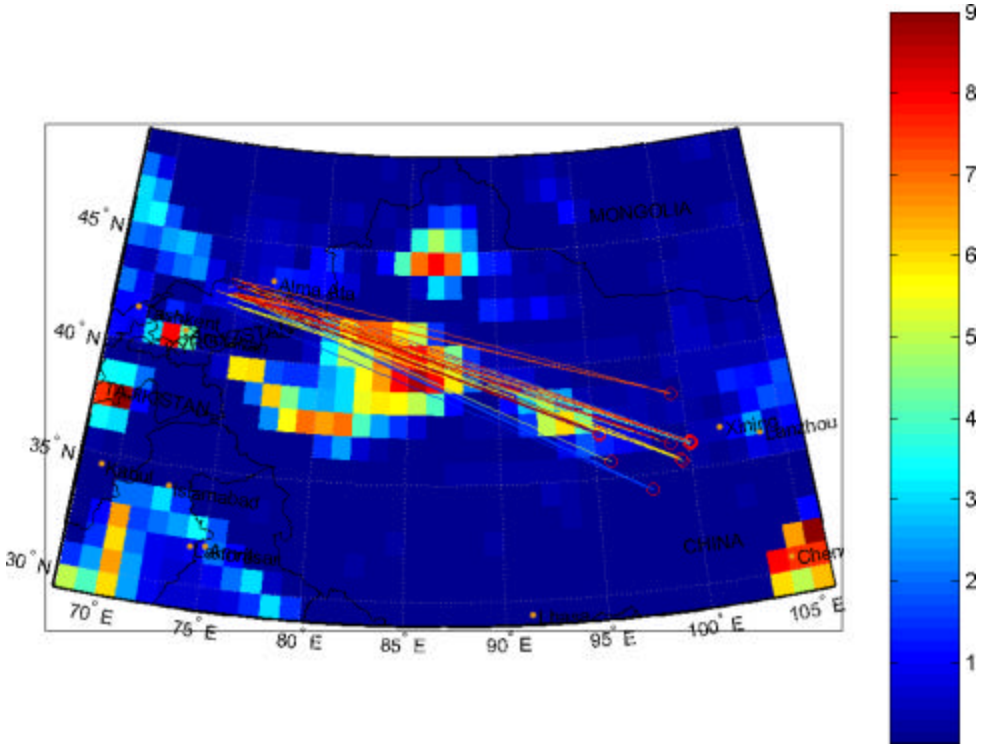

Figure 8. Paths of group velocity dispersion measurements across the Tarim Basin made at the cluster of stations in Kyrgyzstan. The color scale shows sedimentary thickness in kilometers. The ray color corresponds to the dispersion curve color in Figure 7.

Importance of high-frequency data

The higher frequency data is important for measuring low amplitude surface waves at regional distances because most of the observable surface wave energy will be in the higher frequency band. In order to predict the higher frequency dispersion and construct phase-matched filters, it is necessary to have high frequency data to constrain the models. An example is shown in Figure 9. Here we show one dispersion curve for a path running southwest of the Tarim Basin together with the predicted dispersion curve from models determined before and after addition of the new data. Without the high frequency data, the dispersion is determined primarily by the background model, and is nearly flat between 0.05 and 0.1 Hz. With the high frequency data it is clear that there is more variation in the dispersion curve at these higher frequencies, and the model adjusts to match the dispersion data.

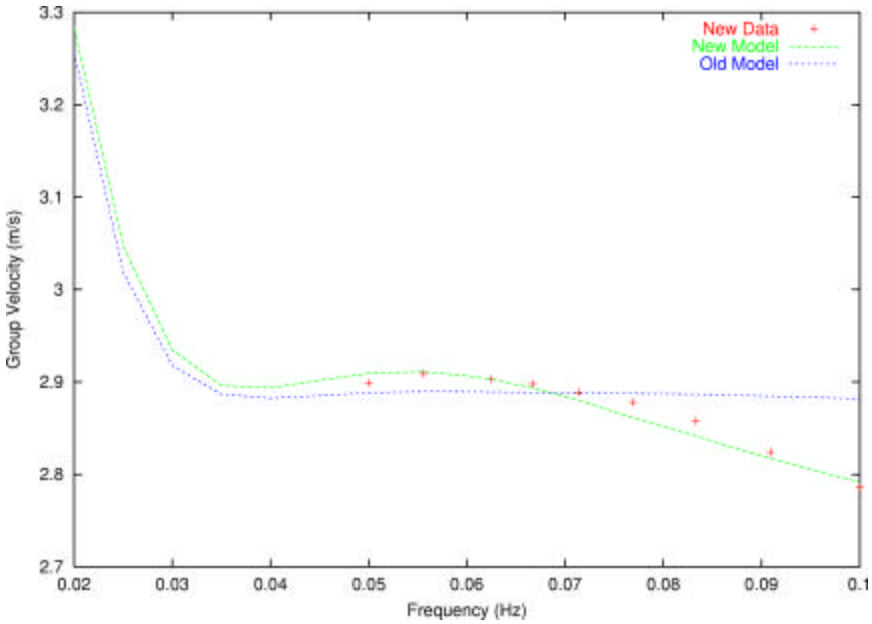

Figure 9. Dispersion curves before and after addition of new high-frequency data.

Plans

This project is nearing its conclusion. CU has completed its database of dispersion curves, tomographic inversions, and development of SSSCs. Most of the remaining effort will be on validation of the results. After completing model development as discussed above, this will be accomplished by applying phase-matched filters derived from this data set to an independent data set of IMS data traversing this region. The data set and inversion results will be delivered to CMR for distribution to other researchers at the end of the project.

CONCLUSIONS AND RECOMMENDATIONS

The high frequency dispersion data set measured by CU provides important information about earth structure and surface wave properties in Central Asia. This level of detail cannot be resolved with more typical lower frequency dispersion data. The Tarim Basin example illustrates how the high frequency surface wave data resolves the fine structure of the earth, and how strongly these structural differences can affect the surface waves. This is important because recovery of low amplitude surface waves through phase-matched filtering depends on accurate prediction of the dispersion. The results of this project will therefore lead to improved capability for identification of surface waves at a lower threshold.

REFERENCES

Bassin, C., G. Laske, and G. Masters, (2000), The Current Limits of Resolution for Surface Wave Tomography in North America, *EOS Trans AGU*, **81**, F897.

Dziewonski, A. M., S. Bloch, and M. Landisman, 1969. A technique for the analysis of transient seismic signals, *Bull. Seism. Soc. Am.*, **59**, 427 - 444.

Dziewonski, A. M., T.-A. Chou, and J. H. Woodhouse, 1981. Determination of earthquake source parameters from waveform data for studies of global and regional seismicity, *J. Geophys. Res.*, **86**, 2825 - 2852.

Kennett, B.L.N., E. R. Engdahl, R. Buland (1995), Constraints on seismic velocities in the Earth from travel times, *Geophys J Int*, **122**, 108-124.

Laske, G., and G. Masters (1997), A Global Digital Map of Sediment Thickness, *EOS Trans. AGU*, **78**, F483.

Laske, G., G. Masters, and C. Reif, Crust 2.0 (2001), A new global crustal model at 2x2 degrees, http://mahi.ucsd.edu/Gabi/rem.html.

Levshin, A. L., V. F. Pisarenko, and G. A. Pogrebinsky (1972), On a frequency-time analysis of oscillations, *Ann. Geophys.*, **28**, 211 - 218.

Levshin, A. L., M. H. Ritzwoller, M. P. Barmin, and J. L. Stevens (2001), Short Period Group Velocity Measurements and Maps in Central Asia, *Proceedings of the 23rd Seismic Research Review*, Vol. I, 258 - 269.

Ritzwoller, M. H., A. L. Levshin, S. S. Smith, and C. S. Lee (1995), Making accurate continental broadband surface wave measurements, in *Proceedings of the 17th Seismic Research Symposium on Monitoring a CTBT*, (ed. J. F. Lewkowicz, J. M. McPhetres, and D. T. Reiter), Phillips Lab., Hanscom AFB, Mass., 482 - 490.

Russell, D. W., R. B. Herrman, and H. Hwang (1988), Application of frequency-variable filters to surface wave amplitude analysis, *Bull. Seismol. Soc. Am.*, **78**, 339 - 354.

Shapiro, N. M. and M. H. Ritzwoller (2002), Monte-Carlo inversion of surface waves (Inversion of broad-band surface-waves with the a-priori information), *J. Geophys. Res.*, in press.

Stevens, J. L., W. L. Rodi, J. Wang, B. Shkoller, E. J. Halda, B. F. Mason, and J. B. Minster (1982), Surface wave analysis package and Shagan river to SRO station path corrections, S-CUBED topical report submitted to VELA Seismological Center, SSS-R-82-5518, April.

Stevens, J. L. and K. L. McLaughlin (2001), Optimization of surface wave identification and measurement, *Pure and Applied Geophysics*, **158**, no. 7, pp 1547-1582.

Stevens, J. L., D. A. Adams, and G. E. Baker (2001), Phase-matched filtering with a one degree dispersion model, *Proceedings of the 23rd Seismic Research Review*, Vol. I, 420 - 430.

Stevens, J. L., D. A. Adams, and G. E. Baker (2002), Improved surface wave dispersion models and azimuth estimation techniques, *Proceedings of the 24th Seismic Research Reveiw*.